JOURNAL OF MATERIALS SCIENCE 26 (1991) 2625–2629

Strength and fracture behaviour of diffusion-bonded joints in Al–Li (8090) alloy

Part II *Fracture behaviour*

D. V. DUNFORD, P. G. PARTRIDGE
Materials and Structures Department, Royal Aerospace Establishment, Farnborough, Hampshire, UK

Al–Li 8090 alloy overlap shear test pieces machined from 3 mm thick diffusion-bonded sheets showed two fracture zones at the bond interface. Zone 1 at the ends of the overlap showed predominantly intergranular fracture and zone 2 at the centre of the overlap showed peel-type fracture. The load appeared to be carried entirely by zone 1. Only zone 1 fracture was obtained in the base metal test piece. The fracture zones were caused by the non-planar stress distribution and by the bending moments associated with this type of test piece. The planar bond interface may accentuate the tendency in these alloys towards low ductility and toughness in the short transverse direction.

1. Introduction

Diffusion-bonded single overlap shear joints in 8090 Al–Li alloy have been shown to have shear strengths similar to that of the base metal (Fig. 1) [1]. The shear strength was independent of overlap length, L, for lengths $L < 3$ mm, but above this value the shear strength decreased with increase in L. This dependence on L has been attributed to the change in elastic stress state from one of almost pure shear to one of mixed shear and normal stresses which gives rise to peel [2].

The shear strengths obtained for diffusion-bonded joints in this alloy depend not only on the quality of the bond interface i.e. on the amount of prior surface oxide and contaminants or residual interface porosity, but also on the fracture mode. It was noted in Part 1 of this paper [1] that intergranular fracture was the dominant fracture mode in the shear test pieces. Part 2 of this paper describes in more detail the fracture morphology in the diffusion-bonded and base metal shear test pieces. The peel strength and fracture behaviour are described in Part 3 [3].

2. Experimental procedure

Al–Li 8090 alloy with a nominal composition (wt %) of Al–2.5Li–1.3Cu–0.8Mg–0.12Zr–0.1Fe–0.05Si was in the form of 2.5 mm thick unrecrystallized sheet or 4 mm partially recrystallized sheet. Single overlap shear test pieces (Fig. 2) were made by diffusion bonding in a vacuum two sheets of identical thickness at 560 °C under platen pressure to give a final overall through thickness deformation of 8% to 12%.

After bonding, a 10 mm long × 5 mm deep section was cut from each edge of the bonded test piece to determine the microstructure before and after a post-bonding heat treatment which consisted of solution treatment (20 min at 530 °C water quench) and ageing (5 h at 185 °C and air cool) to the T6 condition. Surface slots were cut to the depth of the bond line (Fig. 2) to give overlap lengths $L = 1.9$ to 15.1 mm. Similar base metal shear test pieces were made by machining slots to half the sheet thickness after a thermal cycle of 4 h at 560 °C to simulate the bonding cycle followed by STA. Overlap lengths for base metal test pieces were $L = 2$ to 5.3 mm. Fracture surfaces were studied in a Jeol T220 scanning electron microscope (SEM). Test pieces were tested in tension with constraint at a loading rate of 2 kN min^{-1}.

3. Results

In sections through a bonded joint in the unrecrystallized sheet (Fig. 3 in Part 1) the bond interface was indistinguishable from the planar boundaries associated with the pancake-shaped grains in the base alloy. A similar section through a bonded joint in partially recrystallized sheet is shown in Fig. 3; the planarity of the bond interface A–A in this section is in marked contrast to the grain boundaries associated with the equiaxed grains in the base metal at B. However, transmission electron microscopy observations have shown [4] that the bond interface is a conventional large-angle boundary. The planarity of this interface boundary is a characteristic of interfaces produced in aluminium–lithium alloys by solid state diffusion bonding; short segments of straight grain boundary are also a common feature in metallographic sections in this alloy, e.g. at C in Fig. 3, and in transmission electron micrographs [4] of 8090 alloy.

3.1. Shear fracture of diffusion-bonded joints

Macrographs of the fracture surfaces of test pieces with overlap lengths L equal to 2, 4.9 and 15.1 mm are

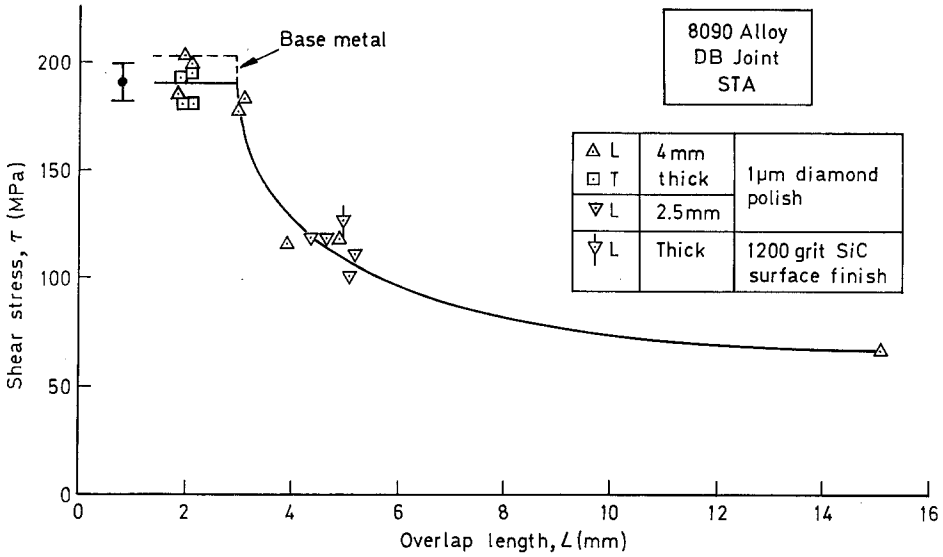

Figure 1 Variation of shear stress with overlap length for diffusion-bonded test pieces.

shown in Fig. 4. For small overlaps (e.g. $L = 2$ mm) the fracture surface topography appears uniform, but for longer overlap lengths, e.g. $L = 4.9$ or 15.1 mm two distinct fracture zones, zones 1 and 2, were visible at the ends and at the centre of the fractures as shown in Fig. 4. The ratio of the length of zone 1 to zone 2 decreased with increase in overlap length, for example

$L = 2$ mm, zone 1 only 2.0 mm

$L = 4.9$ mm, zone 1/zone 2 = 3.1/1.8 mm

$L = 15.1$ mm, zone 1/zone 2 = 5.6/9.5 mm.

SEM fractographs confirmed the surface uniformity in zone 1, as shown in Fig. 5, for $L = 2$ mm. The zone 1 fracture for $L = 15.1$ mm was identical and is shown at higher magnification in Fig. 6a and b. The intergranular fracture surface was very smooth at A but ductile cusps occurred at grain boundary steps at B and are characteristic of a soft precipitate-free zone [5]. Occasional voids were also observed within grains or at grain boundaries, e.g. at C in Fig. 6a; these could be associated with coarse Fe–Cu- or Mg–Cu-rich insoluble particles in the alloy [6].

Zone 2 was characterized by a much rougher surface topography caused by a mixture of inter- and transgranular shear fracture (Fig. 7) and areas of pull-out. The latter were caused by cracks deviating from the bond interface and propagating in both trans- and intergranular modes in planes parallel to the bond interface. This led to large depressions or mounds on the fracture surfaces with dimensions in a direction

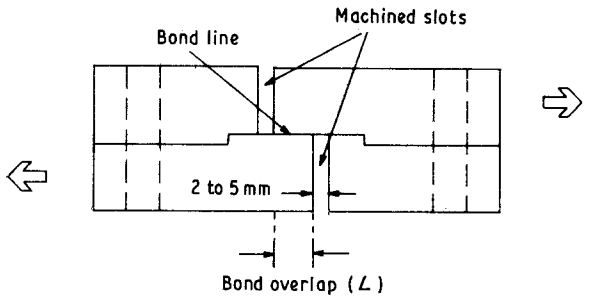

Figure 2 Schematic diagram of diffusion-bonded overlap shear test piece.

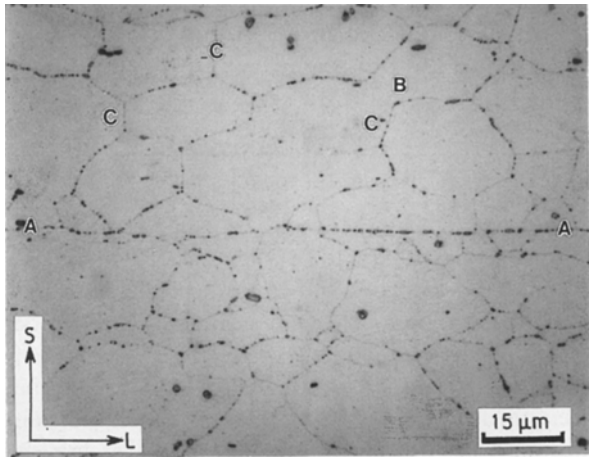

Figure 3 Section through diffusion-bonded joint in partially recrystallized 4 mm thick sheet in STA condition.

normal to the surface of at least two grain diameters; a typical example associated with extensive shear for the test piece with $L = 4.9$ mm is shown at A, Fig. 8a and b, and an example of pull-put with little shear is shown at B, Fig. 8a and c.

3.2. Shear fracture in the base metal

When $L > 3.1$ mm, tensile failure occurred in the base metal but peel occurred in the bonded joint; this suggests that the peel resistance was greater for the base metal. The shear fracture obtained when $L = 2$ mm is shown in Fig. 9. At low magnification the surface roughness appeared much greater than for the corresponding diffusion-bonded joint, compare Figs 5 and 9a, but at higher magnifications smooth fracture areas were apparent with diameters of about 20 to 50 μm at A in Fig. 9b; these dimensions correspond to the grain diameters for this alloy (Fig. 3). In a section through the bonded shear test piece shown in Fig. 10a fracture has occurred along the bond interface at A–A and partly through the base metal at the base of the machined notch at B–B. In a similar test piece the base metal crack B–B turned through 90° and intercepted the bond interface fracture plane as shown in Fig. 10b. This enabled a direct comparison to be made between

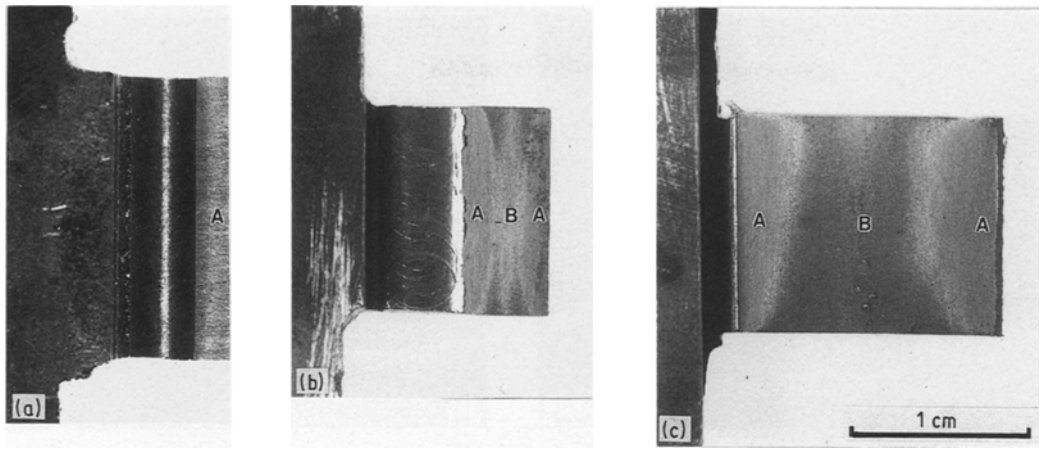

Figure 4 Shear fractures of diffusion-bonded joints in STA condition. Overlap length, L (mm); (a) 2, (b) 4.9, (c) 15.1. Fracture zone 1 at A and zone 2 at B.

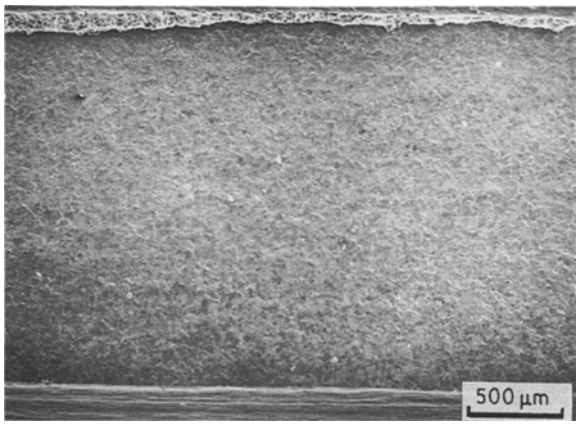

Figure 5 Scanning electron micrograph of Zone 1 fracture in diffusion-bonded joint, $L = 2$ mm. Shear test direction is from top to bottom in Figs 5 to 7.

the fractures in the planar bond interface at C and in the base metal at D; the greater roughness for the fracture in the base metal is apparent.

3. Discussion

In both the DB interface and the base metal, intergranular fracture was the dominant failure mode. The difference in fracture surface roughness was related primarily to the grain-boundary surface contour. Mounds and cavities on the zone 2 fracture surfaces were caused by metal pull-out. These results and those in Part 1, together with the TEM observations [4], are consistent with parent metal strength and a conventional grain-boundary microstructure in the bond interface.

Intergranular fracture is common in commercial Al–Li 8090 and 2090 alloys which tend to have well-developed pancake-shaped grains with their major axes parallel to the rolling plane [5, 7, 8]. This microstructure led to intergranular delamination, and low tensile ductility and fracture toughness in the S–T and S–L orientations in these alloys. These results suggest that the mechanical properties of the bonded joints may be limited by the planar boundary oriented normal to the short transverse direction.

The reduction in the measured "shear" strength with increase in overlap length has been observed for other DB aluminium alloy joints [2], for brazed joints [9, 10] and for adhesive-bonded joints [11–13]. The elastic stress distribution for this type of overlap joint is complex and most analyses have been carried out for adhesive-bonded joints [11–13]. The stresses are sensitive to the moment factor, which is dependent on the test piece, the shear test and the sheet thickness. However, the stress distribution characteristic of an overlap test piece consists of a very high tensile stress (about 4 × applied stress) normal to the bond interface at the ends of the bonded length where the shear stress is zero, a region of high shear and low tensile stress within a distance $L < t$ from the ends of the bond and a region at the centre of the bond length where the stresses are zero. In the present tests the constraint imposed by the shear test jig may reduce the tensile component at the end of the bond [14].

At the end of zone 1 fracture the ratio of resolved normal force/bond width values obtained for the measured bend angles of 3° to 5° are 31 to 88 $N\,mm^{-1}$ for the 4.9 and 15.1 mm overlaps; these values are in good agreement with measured 90° peel strength values of 31 to 48 $N\,mm^{-1}$ [3]. Taking zone 1 bond areas only, shear strength (load/area) values of 190 and 181 MPa are obtained for the 4.9 and 15.1 mm overlaps, respectively. The values are within the shear strength scatter band obtained in the plateau region for $L = 2$ mm in Fig. 1. These results suggest that the central region contributes little to the shear strength of the joint.

It is therefore concluded that the fractures observed in the present tests are consistent with crack nucleation at the ends of the joint caused by the high tensile stress, followed by fast crack growth through zone 1 to relax the shear strains (Fig. 11a and b). The crack growth rate may fall as the crack enters the region of low stress and plastic bending and an increased normal stress component causes peel-type fracture in zone 2, as shown schematically in Fig. 11c. Even if the high rate of intergranular crack growth in zone 1 is used to explain the lack of deformation on this fracture surface, it is difficult to reconcile the fracture

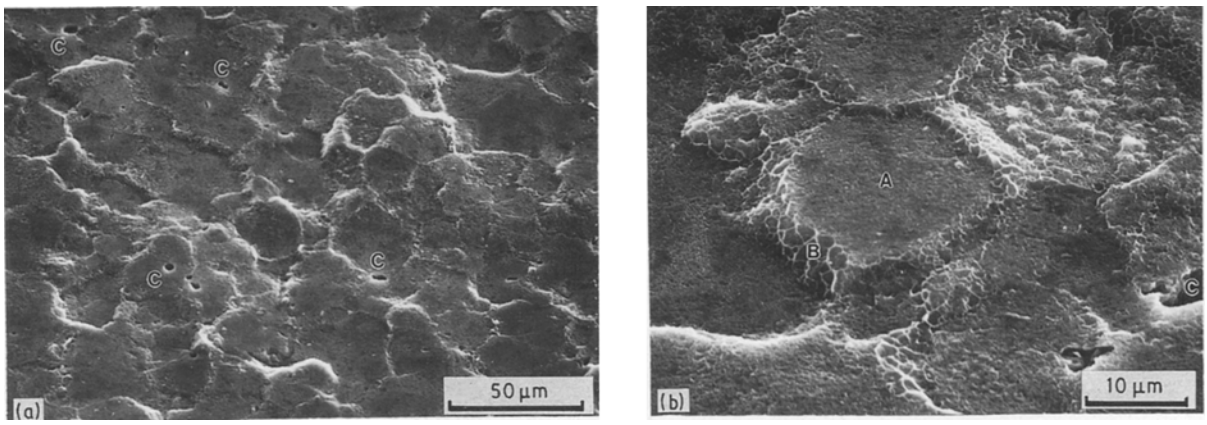

Figure 6 Scanning electron micrograph of Zone 1 fracture in diffusion-bonded joint, $L = 15.1$ mm.

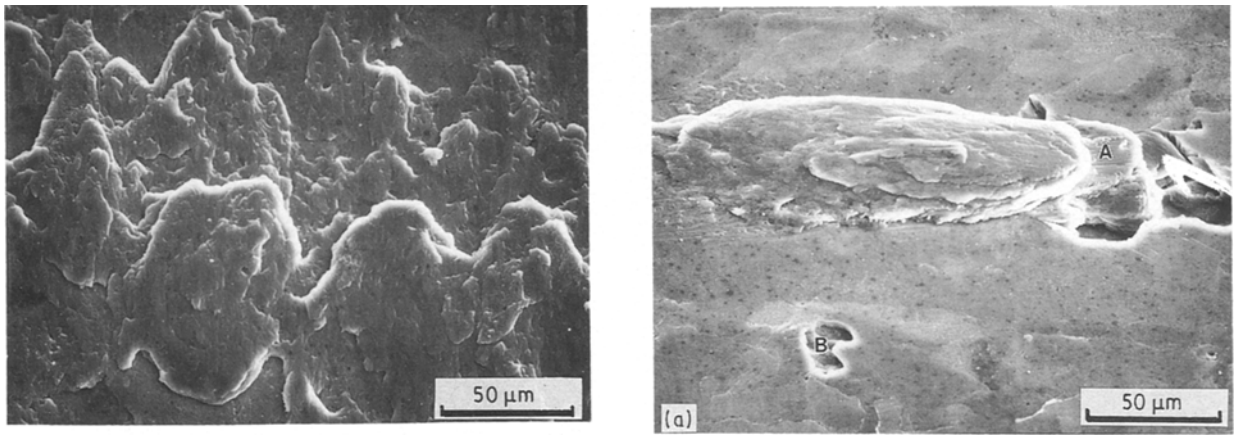

Figure 7 Scanning electron micrograph of Zone 2 fracture in diffusion-bonded joint, $L = 15.1$ mm.

morphology with shear; it is possible that the local crack tip stresses actually give rise to tensile fracture in zone 1.

Diffusion bonding is a particularly attractive joining technique for metal matrix composites (MMCs), but the much greater stiffness associated with these materials is likely to change significantly the elastic stresses and strains in such joints. There is clearly a need for a more rigorous stress analysis based upon fracture mechanics of these types of joint in metals and in MMCs.

4. Conclusions

The fracture of overlap shear test pieces in Al–Li 8090 alloy was similar for both the base metal and the diffusion-bonded joints. Intergranular fracture was the dominant failure mode but two types of fracture surface were observed as the theoretical elastic stress state changed from that approximating to shear to that characteristic of peel. The planar bond interface may accentuate the tendency in these alloys towards low ductility and toughness in the short transverse direction.

Acknowledgement

This paper is published by permission of The Controller, Her Majesty's Stationary Office, holder of Crown Copyright.

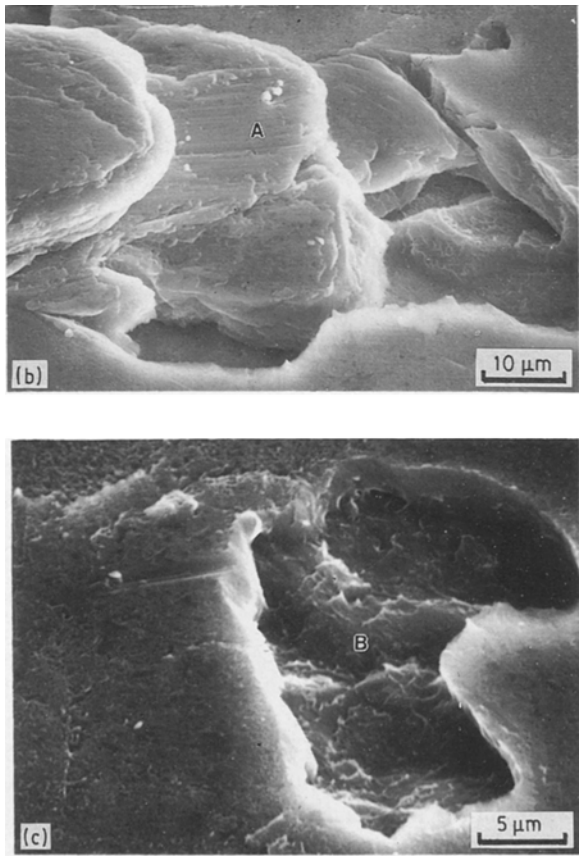

Figure 8 Scanning electron micrograph of Zone 2 fracture in diffusion-bonded joint, $L = 4.9$ mm. Shear test direction is from left to right.

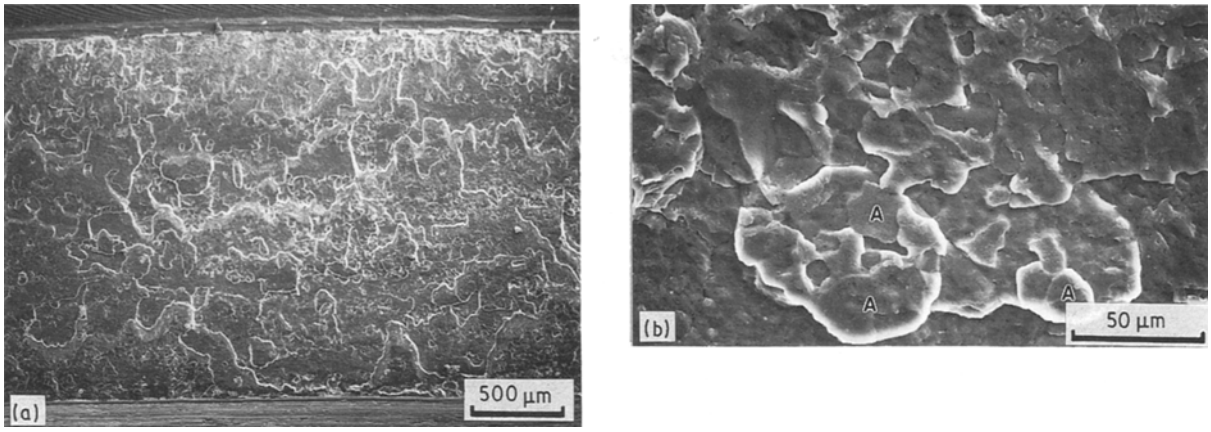

Figure 9 Scanning electron micrograph of Zone 2 fracture in base metal, $L = 2$ mm. Shear test direction is from top to bottom.

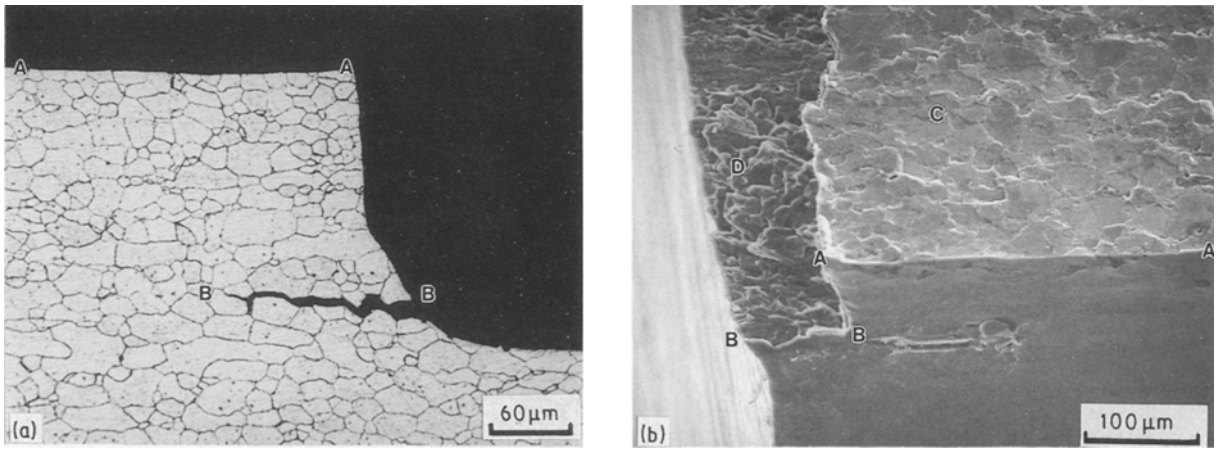

Figure 10 Fractures in diffusion-bonded joint, $L = 2$ mm. (a) Zone 1 bond interface fracture at A–A, base metal fracture at A–A, base metal fracture at root of slot at B–B. (b) Scanning electron micrograph of base metal fracture at root of slot at D, zone 1 bond interface fracture at C.

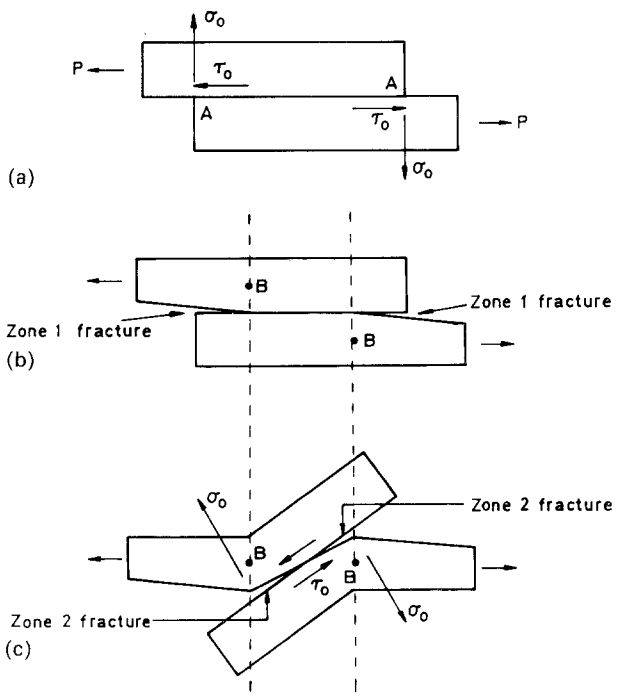

Figure 11 Schematic diagram of fracture and deformation of an overlap shear test piece, P = applied force, σ_0 = normal (peel) stress, τ_0 = shear stress A–A bond interface, B = plastic hinge.

References

1. D. V. DUNFORD and P. G. PARTRIDGE, *J. Mater. Sci.* (1990) 4957.
2. P. G. PARTRIDGE and D. V. DUNFORD, *ibid.* **22** (1987) 1597.
3. *Idem., ibid.* unpublished work.
4. C. J. GILMORE, D. V. DUNFORD and P. G. PARTRIDGE, *J. Mater. Sci.* (1991) in press.
5. K. T. V. RAO and R. O. RITCHIE, *Mater. Sci. Technol.* **5** (1989) 882.
6. N. J. OWEN, D. J. FIELD and E. P. BUTLER, "Aluminium–Lithium III", Proc. Int. Cong., Oxford, England, 1986 (Inst. Metals) p. 576.
7. D. DEW-HUGHES, E. CREED and W. S. MILLER, *Mater. Sci. Technol.* **4** (1988) 106.
8. A. F. SMITH, "New light alloys", AGARD Conference Proceedings No. 444, Paper 19 (AGARD, France, 1988).
9. N. BREDZ and F. M. MILLER, *Welding J. Res. Suppl.* **47**, 11 (1968) 481.
10. J. R. SPRINGARN, *ibid.* **68** (1987) 99.
11. E. LUGSCHEIDER, H. REIMANN and O. KNÒTEK, *ibid.* **56**(6) (1977) 189.
12. A. J. KINLOCH, *J. Mater. Sci.* **17** (1982) 617.
13. L. J. HART-SMITH, "Delamination and debonding of materials" ASTM STP 876 (American Society for Testing and Materials, Philadelphia, Pennsylvania, 1985) p. 238.
14. A. D. CROCOMBE, personal communication, 1988.

Received 8 January
and accepted 1 February 1990